Thermal Properties of Acylated Low Molecular Weight Chitosans

[1]Shu Xian Tiew and [2]Misni Misran*
[1,2]*Department of Chemistry, Faculty of Science, University of Malaya, 50603 Kuala Lumpur, Malaysia.*
misni@um.edu.my*

Summary: Acylated low molecular weight chitosans (LChA) were prepared from nucleophilic acylation of chitosan using acid anhydrides of short and medium chain length (4 - 10) to study the response of applied heat as a function of acyl chain length. Thermogravimetric analysis (TGA) revealed the decomposition of LChA consisted of glucosamine and acyl-glucosamine units around 141 - 151°C to 400 - 410°C. Both TGA and differential scanning calorimetry (DSC) analyses indicated that the introduction of acyl groups disrupted the hydrogen bonding of chitosan, the effect was more prominent as the degree of substitution and chain length of LChA increased. Grafting of acyl chains lowered the kinematic viscosity of LChA as the disruption of hydrogen bonding led to decreased hydrodynamic volume. Field emission scanning electron micrographs showed that LChA with longer chains having larger particle size due to bigger occupancy volume of acyl chains during spray drying.

Keywords: Chitosan, Modification, Chain length, Thermal properties, Hydrogen bonding.

Introduction

Hydrophobically modified chitosan (HMC) as a unique structure to bear both hydrophobic and hydrophilic segments on the chitosan backbone have been studied intensively on their designs and biological potentials for drug delivery [1-3] and biomedical applications [4, 5] in the form of micelles [6], polymeric vesicles [7], ionic liquids [8], hydrogels [9], films [10], and fibers [11]. The self-aggregation of HMC as drug carrier is attributed to the interaction of hydrophobic groups at the core while facing the hydrophilic portions with polar water to reduce the interfacial tension.

The modifications of chitosan by the introduction of hydrophobes of different chain length not only produce new macromolecular conformations that change the chemical structure, but also influence the physical properties of the chitosan such as water solubility, critical aggregation concentration, and particle size, especially when dealing with heat [12, 13]. The effect of temperature alteration to HMC is important to reveal their conformation, phase transition and degradation towards temperature, thus a better knowledge on the thermal properties of HMC is advantageous in the fabrication of HMC for desirable applications, as well as for processing optimization, storage, and transport purposes. For instance, the spray drying of HMC at high temperature can transform it into powder for the sake of convenience and cost-effectiveness of transportation and storage. HMC with known thermal properties offers basic and opportunities for the fabrication with other modes of drug delivery or

biomedical engineering, which may exist in the form of chitosan fiber, film, hydrogel, and nanocrystal.

Previous studies showed that the Schiff based (aromatic aldehydes derivatives)[14], lactic and glycolic acid grafted chitosan [15] are less thermally stable compared to the native chitosan as a consequence of the substitution of the free amino group by the substituents. Similarly, it was observed a decreased thermal stability of the aliphatic alkyl chain palmitoyl chitosan[16]. Despite this, the thermal stability of palmitoyl and *N*-phthaloyl chitosan [17] increased with a higher degree of substitution which was attributed to the formation of a stronger hydrophobic interaction between the alkyl chains. The degree of substitution not only plays role in the thermal stability, chain length of the hydrophobes is also the key factor affecting stability. Choi *et al*. (2007) [18] reported that a longer hydrocarbon chain contributed to a higher spatial organization of the polymer and hence provided a higher thermal stability. This is similar to the study of Le Tien (2003) [19] which found that the hydrophobic interaction formed from the self-assembly association of longer acyl chain length (C8-14) could stabilize the chain organization.

The purpose of this study is to investigate the effects of introducing hydrophobic acyl groups with different chain length on the thermal properties of low molecular weight chitosan. Low molecular weight chitosan was selected because of its solubility in an aqueous environment. Acylated chitosans were prepared via acylation with short acyl groups such as

---

butyryl and hexanoyl and also medium acyl groups included octanoyl and decanoyl onto low molecular weight chitosan (25 kDa). The degree of substitution (DS) of acylated chitosans was determined by acid-base titration in order to correlate the structural modification to the thermal behaviors in thermogravimetric analysis (TGA), differential scanning calorimetry (DSC) and viscosity. The morphology of acylated chitosans after spray drying was observed using field emission scanning electron microscopy (FESEM).

Experimental

Materials

All the chemicals and reagents used in this study were analytical grade and prepared using deionized water with a resistivity of 18.2 Ω/cm that was purified using Barnstead Diamond Nanopure water Purification unit equipped with Barnstead Diamond™ RO unit (Barnstead International, Iowa, USA). Chitosan with an average molecular weight of 150 kDa was supplied by Acros Organics (New Jersey, USA). Acid anhydrides including butyric anhydride and hexanoic anhydride were purchased from Sigma-Aldrich (St. Louis, MO, USA) and Merck (Darmstadt, Germany) respectively, whereas octanoic and decanoic anhydride were purchased from TCI America (Portland, Oregon, USA). Solvents and acids such as acetic acid, hydrochloric acid (HCl) (37%), methanol and acetone were supplied by Merck (Darmstadt, Germany) as well, whereas sodium hydroxide (NaOH) was obtained from Friedemann Schmidt Chemicals (Parkwood, WA, Germany).

Synthesis of Acylated Chitosans

Low molecular weight chitosan (LCh of 25 kDa with a degree of acetylation =12.5%) was prepared as reported previously and dissolved in acetic acid and methanol at 1:1 ratio (v/v) before pH adjustment to 7 [20]. Butyric anhydride, hexanoic anhydride, octanoic anhydride and decanoic anhydride were added to their individual chitosan solutions in different mole ratios to the glucosamine unit of chitosan under magnetic stirring and left to react overnight. The chitosan mixtures were then neutralized, filtered, precipitated with acetone and then centrifuged at 10,000 rpm at 25 ℃ for 3 minutes. The collected chitosans were washed with excess methanol to remove excess fatty acid prior to drying in a vacuum oven over silica gels. The acylated chitosans (LChA) were labeled based on the acyl chain length and mole ratio, for example,

LChC4-M.8 was chitosan acylated with butyryl group at a mole ratio of 1:0.8.

Characterizations of LCh and LChA

Determination of the degree of substitution (DS) by acid-base titration

The determination of the degree of substitution (DS) of ChA was carried out using acid-base titration. LCh and LChA dissolved in their respective HCl solution were titrated with 0.5 mol dm^{-3} NaOH solutions under magnetic stirring and the volume of added NaOH was recorded. The pH change of chitosan upon titration with NaOH was measured using a Cyberscan 510 pH meter calibrated with pH 4.01, 7.00, 10.01 ($\pm$ 0.02) buffer standard solutions at 25 °C. The titration was stopped when the solution reached pH 11.0. The NaOH solution used was standardized with potassium hydrogen phthalate (KHP) using phenolphthalein as the indicator. The pH curve as a function of added NaOH solution was plotted and the degree of deacetylation (DD) was calculated based on the difference between first and second inflection point from the titration derivatized graph ($\Delta pH/\Delta mL$) using the equation shown below [21]. Degree of acylation (DA) and degree of substitution (DS) of LChA were then calculated based on the average of triplicates:

$$DD\ (\%) = \frac{203.20 \times w\ (NH_2)}{16.02 + 0.42 \times w\ [(NH]_2)}$$

$$w(NH_2)\ (\%) = \frac{v \times c \times 100 \times 0.016}{w_{dry}}$$

$$DA\ (\%) = (100 - DD)(\%)$$
$$DS\ (\%) = DA_{LCh} - DA_{LChA}$$

where V was the volume of NaOH added between two abrupt changes of pH, c was the concentration of NaOH solution and w_{dry} was the dry weight of chitosan sample in percentage (derived by excluding the moisture content in TGA analysis), 203.20 was the molecular weight of chitin monomer, 16.02 was the molecular weight of amino group of chitosan, 0.42 was the coefficient calculated from the difference between molecular weight of chitin and chitosan monomer units respectively.

Thermogravimetric analysis (TGA)

Approximately 2 - 3 mg of LCh and LChA were placed in a ceramic pan and heated at a rate of 10 °C min^{-1} from 35 to 900°C using Perkin Elmer

Pyris 6 Thermogravimetric Analyzer (USA) under a nitrogen purge at 50 mL min^{-1}.

Differential scanning calorimetry (DSC)

DSC was carried out by weighing approximately 5 mg of LCh and LChA in hermetic aluminium pans with covered lids and heated at a rate of 5 °C min^{-1} from 30 to 300°C in a nitrogen atmosphere of 50 °C min^{-1} by using TA Instruments model Q20 calorimeter (Perkin-Elmer, USA). The calorimeter was calibrated using indium and a blank aluminium pan with lid was used as a reference.

Kinematic viscosity

The kinematic viscosity of LCh and LChA was measured at 20, 30, 40, 50, 60, 70 and 80°C using a Cannon Ubbelohde Capillary No 1c and Lauda S5 measuring stand in Lauda E200 water bath (Lauda Scientific GmbH, Germany). Kinematic viscosity was determined based on the time that took the samples to flow from an upper etched mark to a lower mark of the viscometer as recorded by the Lauda PVS 1/4 software and the results were reported as the average of three measurements based on the equation below:

$$v = K (t - \theta)$$

where v was the kinematic viscosity, K was the viscometer constant, t was the time flow between two etched marks of viscometer, θ was kinetic energy correction of viscometer respectively.

Field emission scanning electron microscope (FESEM)

LCh and LChA were spray dried at an inlet temperature of 130°C using a Mini Spray Dryer Model 290 (Buchi Labortechnik AG, Flawil, Switzerland). The chitosan powder was put on the double sided adhesive tape fixed on the metal stub and observed using FEI Quanta 450 field emission scanning electron microscope (FESEM) (Hillsboro, Oregon, USA).

Results and Discussion

Reaction

Acylated low molecular weight chitosan were synthesized from the nucleophilic acyl substitution reaction of chitosan and acid anhydrides include butyric, hexanoic, octanoic and decanoic anhydride, as shown in the Fig. 1 [19], which were

later named as butyryl (LChC4), hexanoyl (LChC6), octanoyl (LChC8) and decanoyl (LChC10) chitosan, respectively.

R : $(CH_2)_nCH_3$, n= 2, 4, 6, 8
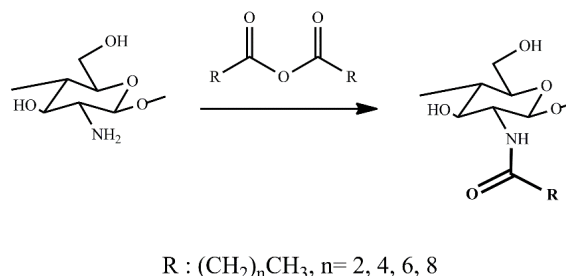
Fig. 1: Chitosan derivatives obtained from the acylation of chitosan with acid anhydrides.

Determination of degree of substitution (DS)

Fig. 2 presented the acid-base titration curve and the derivatized plot of LCh. There were two inflection points in the titration derivatized plot; where the first inflection point indicated the volume of NaOH solution needed to neutralize the excessive HCl in the solution, and the second inflection point revealed the equivalence point of the protonated chitosan. The DS was calculated from the difference between these two inflection points which gave the moles of protons needed to protonate the free amine groups, thus corresponding to the number of glucosamine units of chitosan [22]. From Fig. 3, it can be observed that increasing of acid anhydrides caused a higher DS value of the LChA. The increase of the DS of short chains acylated chitosans such as LChC4 and LChC6 (8.0 – 18.0%) was higher than those with longer chains LChC8 and LChC10 (1.5 – 12.0%). This was probably due to the steric hindrance effect caused by the longer acyl chains that prevented the attack by the nucleophilic amino group of LCh.

TGA thermograms were presented in the form of percentage of weight loss and the respective derivative versus temperature as shown in Fig. 4(a) and 4(b). There were three main weight losses showed in TGA thermograms for LCh and LChA, the first was the elimination of adsorbed water moisture (W1) from the beginning of the heating process until a temperature of 140 - 150°C was reached. As compared to the weight loss of LCh at 3.6%, LChA exhibited higher weight loss at 8 - 13% as more moisture was trapped within weaker hydrogen bonding of chitosan after acylation (Fig. 5). The random attachment of acyl groups onto chitosan loosen the packaging arrangement of chitosan and facilitated the water penetration into the chitosan

network. In LCh, there was a higher number of hydrogen bonds formed between hydroxyl and amino groups in the polymer chains, thus less amount of amino groups were available to form hydrogen bonding with water molecules from the moisture. For this reason, the maximum degradation temperature of moisture of LCh obtained from the curve of derivative of weight loss percentage was 97°C, which was higher than those of LChA around 53 - 66°C. The moisture loss of LChC4 and LChC6 at 8 - 10%

was lower than LChC8 and LChC10 at 8 - 13%, which could be explained by two possibilities. First, the higher DS of LChC4 and LChC6 reduced the number of free amino groups that could form hydrogen bond with water. Secondly, the bulkier LChC8 and LChC10 sterically hindered the intramolecular and intermolecular interaction between polymer chains, therefore the chitosan was more susceptive to moisture.
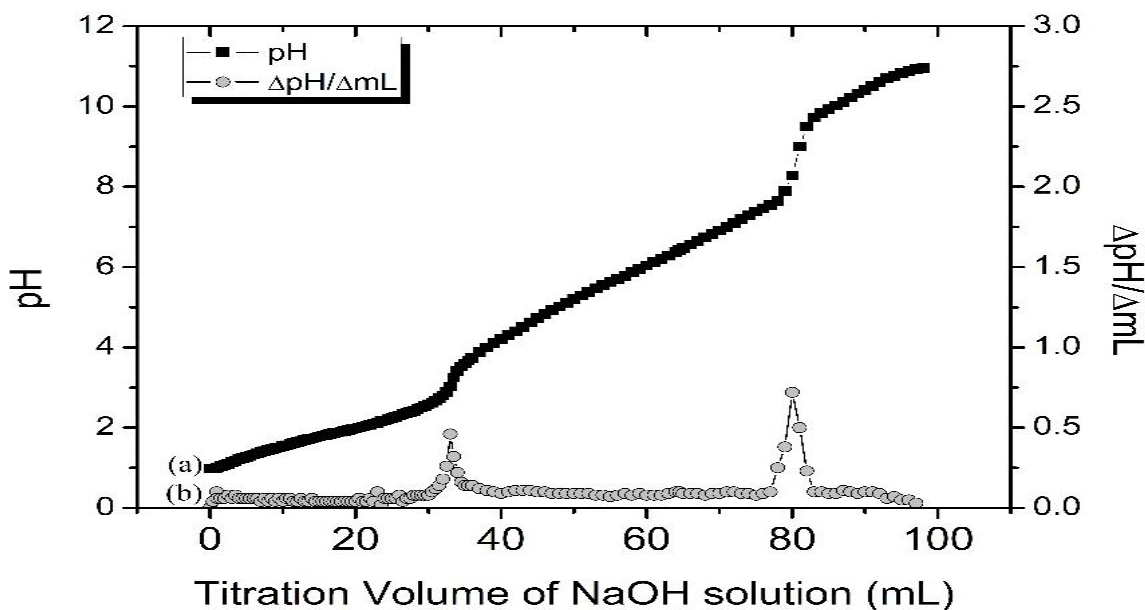
Fig. 2: Curve (a) indicated acid-base titration and curve (b) indicated the derivatized plot of LCh where the difference between the two inflection points was used in the determination of DD.
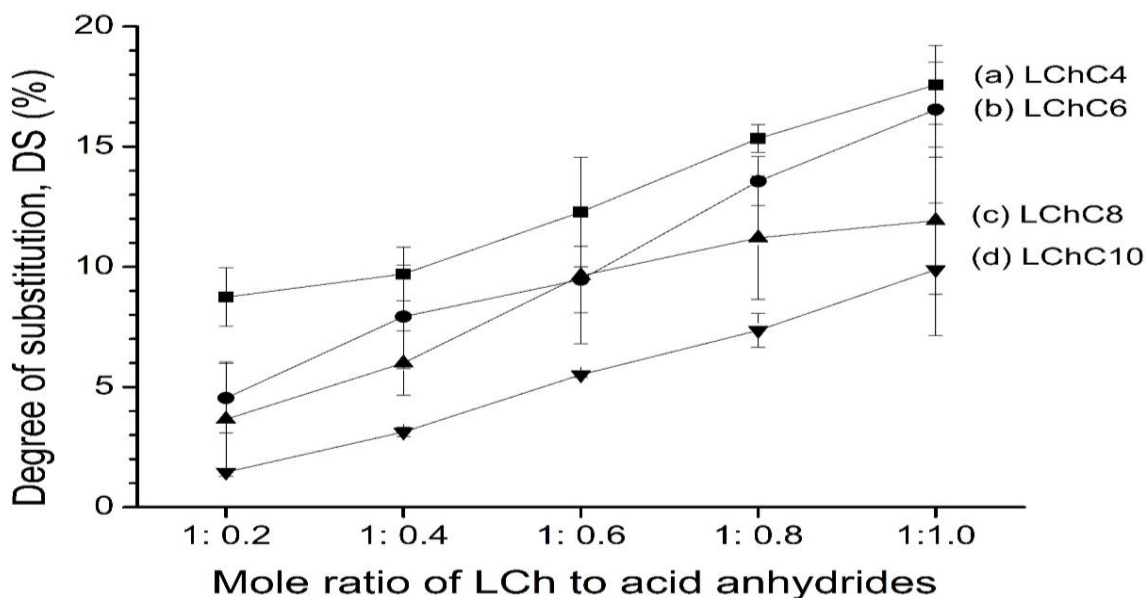
Fig. 3: Degree of substitution (DS) of LChA for acylation at different mole ratio of LCh to acid anhydrides.

Thermogravimetric analysis (TGA)

The second thermal degradation was the major weight loss (W2) of chitosan, and it occurred in the steep region from 141 - 151°C to 400 - 410°C (Fig. 4(a) and 4(b)). This significant weight loss of chitosan was due to the decomposition of the chitosan main chains [17, 23]. It can be seen in Fig. 5 that LChC4, LChC6 and LChC8 showed a higher amount of weight loss at 43.0 – 53.0% as compared to weight loss of LCh at 41.0% during this stage. This was probably due to the decomposition of more chitosan constituents of LChA including glucosamine, *N*-acetyl-glucosamine and acyl glucosamine as compared to LCh that consist of only glucosamine and *N*-acetyl-glucosamine subunits. Therefore, the weight loss was more pronounced as the DS of LChA increased. LChC10 showed the lowest weight loss at 41.1 – 43.0% among LChA due to its low DS. The two peaks presented in the thermogram of derivative of weight loss percentage in Fig. 4(b) described the decomposition of chitosan

main backbone, where the first peak started around 141 - 151°C to 260 - 270°C, the second peak started around 261 - 271°C to 400 - 410°C showed a deeper depression as the DS increased. It was suggested that the first peak is related to the decomposition of glucosamine and the second peak is related to the decomposition of acyl glucosamine of chitosan, this agreed with the DSC study by Guinesi and Cavalheiro [24] in which the decomposition of glucosamine occurred before the decomposition of *N*-acetyl-glucosamine of chitosan. This indicates that glucosamine possesses lower thermal stability, which could be attributed to the lower molecular weight of glucosamine subunits (161 g mol^{-1}) as compared to acyl glucosamine subunits of chitosan such as butyryl chitosan at 231 g mol^{-1}, hexanoyl chitosan at 259 g mol^{-1}, octanoyl chitosan at 287 g mol^{-1} and decanoyl chitosan at 315 g mol^{-1}. The last stage of weight loss after 400 - 410°C was the degradation of the residual inorganic complex of nitrogen, carbon and oxygen contents [25].
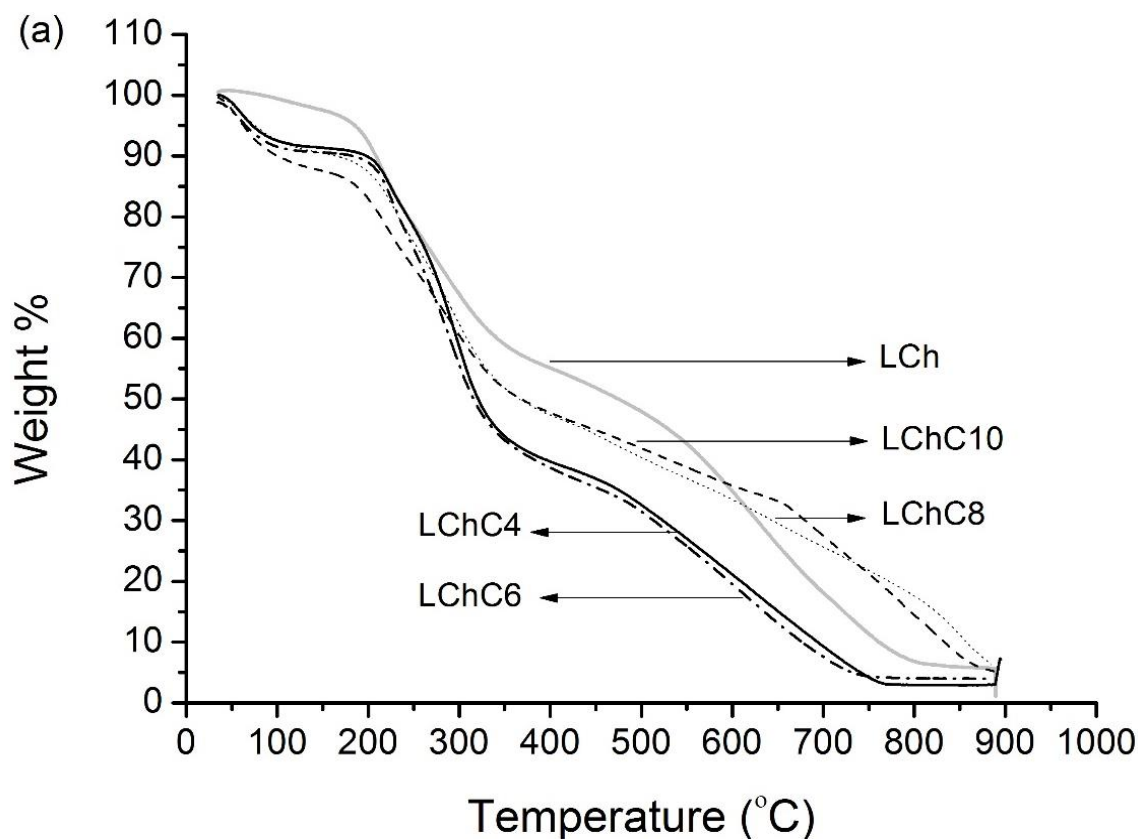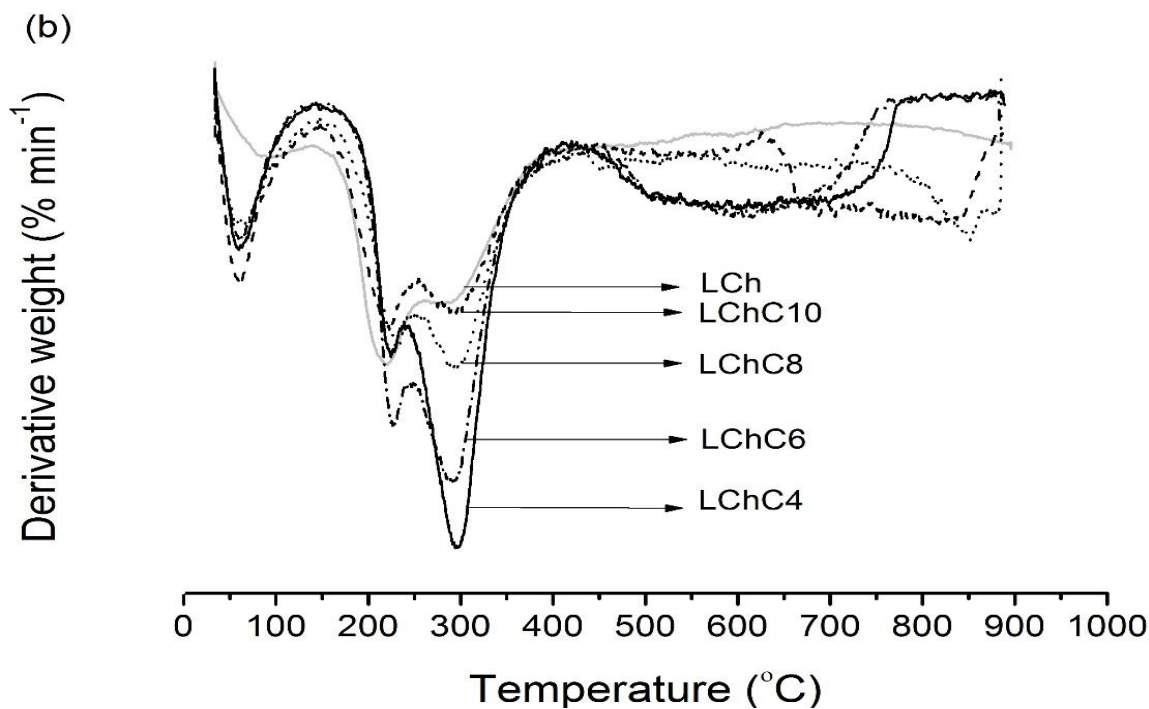
Fig. 4:   (a): Thermogravimetric thermogram and (b) derivative thermogravimetric thermogram of LCh and LChA.
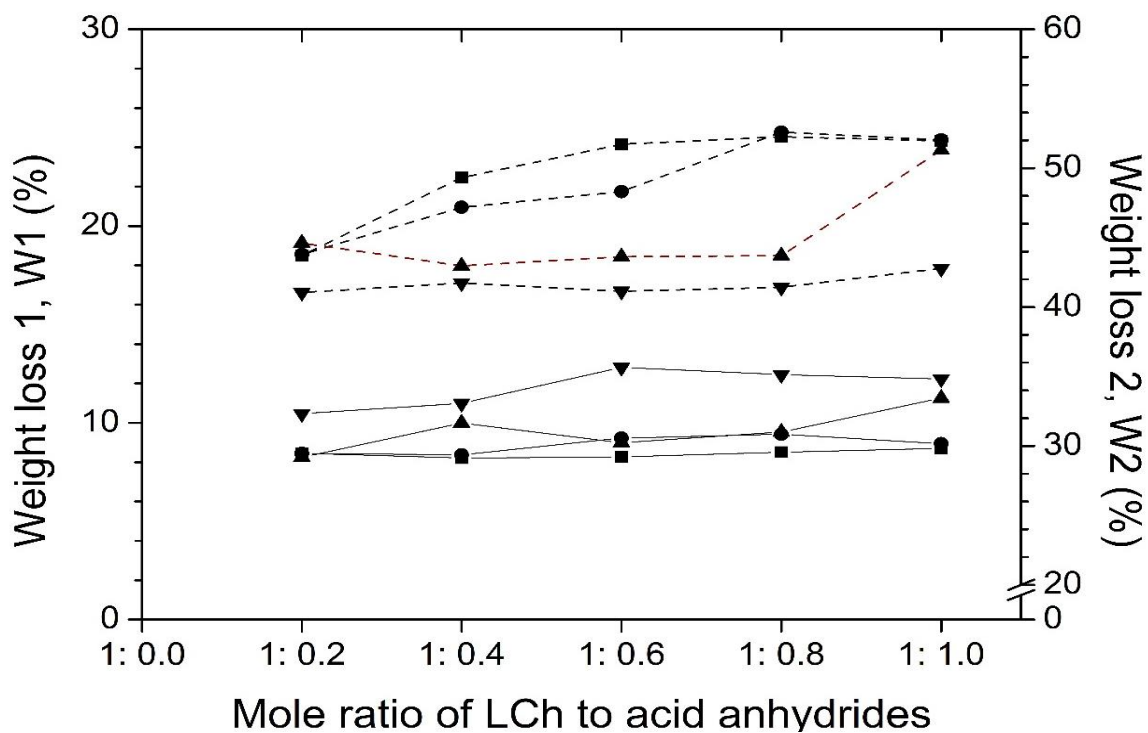
Fig. 5:   Weight loss of LChC4 (■), LChC6 (●), LChC8 (▲) and LChC10 (▼) in the first stage (W1) which indicated by solid line and second (W2) stage of decomposition in the TGA thermogram which represented by dashed line.

Differential Scanning Calorimetry (DSC)

The DSC curve of both LCh and LChA was shown in Fig. 6. As compared to LChA, LCh showed an exothermic peak around 140 - 175°C which may be attributed to the decomposition of the glucosamine of chitosan [24]. The exothermic peak diminished after acylation as less amino groups of chitosan were detectable in LChA. LCh showed a prominent and intense endothermic peak at a peak temperature of 176.4°C. A similar endothermic peak value was also reported by Zeng, Fang [26] and Chuang, Young [27], which was at 179.4°C and 180°C respectively, it was identified as the dissociation process of interchain hydrogen bonding of chitosan. The peak temperatures of LCh (176.4°C) shifted to a lower temperature after acylation as the acyl chains attached disrupted the hydrogen bonding within chitosan, this effect was more prominent with longer acyl groups, as shown in Fig. 7(a). Hence, LChC4, LChC6, LChC8 and LChC10 showed a decreasing endothermic peak temperature of 168.1, 166.4, 159.2 and 159.9°C respectively (Fig. 6).

The heat enthalpy of the endothermic peak was higher in the LChA than in LCh (160 J g^{-1}). This may be attributed to the correlation between the water holding capacity and the chemical and supramolecular structures of the chitosan [28, 29]. Fig. 7(b) showed that short chains of LChC4 exhibited decreasing heat enthalpy, this is a possible consequence of the decreasing of hydrogen bonding with increased DS. As the chain length increased to more than six carbon atoms with increasing DS, the hydrogen bonding of amino and hydroxyl groups of LChC6, LChC8 and LChC10 was disrupted greatly and it became more susceptible to moisture by forming hydrogen bonding with water molecules, with increasing enthalpy indicated from the broad endothermic peak. This is supported by the increase of moisture weight loss in the TGA thermogram (Fig. 5). From Fig. 7(a), it can be seen that LChC4 and LChC6 with lower moisture content showed a higher peak temperature compared to LChC8 and LChC10, the effect was prominent from a mole ratio of 1:0.6 onwards. The high heat enthalpy of LChC8 and LChC10 at a mole ratio of 1:0.2 may be due to their close packing with stronger hydrogen bonding at low DS (Fig. 7(b).
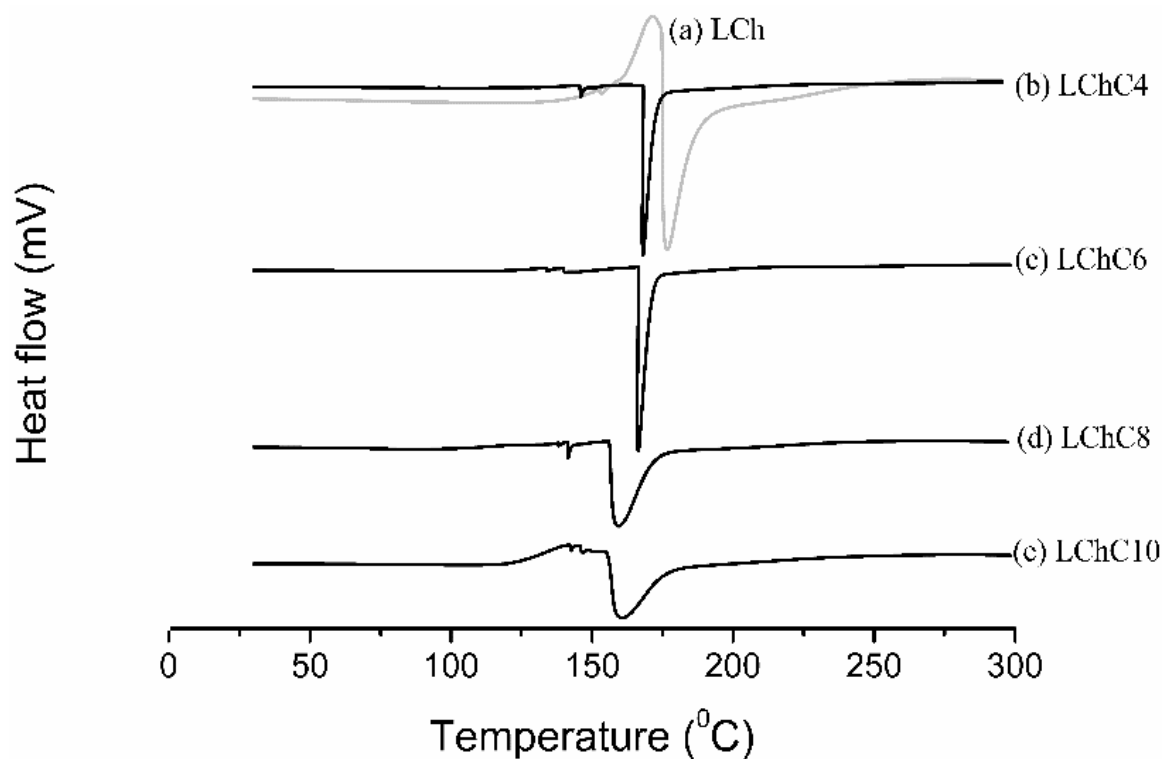
Fig. 6: DSC curve of LCh and LChA during heating from 30 - 300 °C.
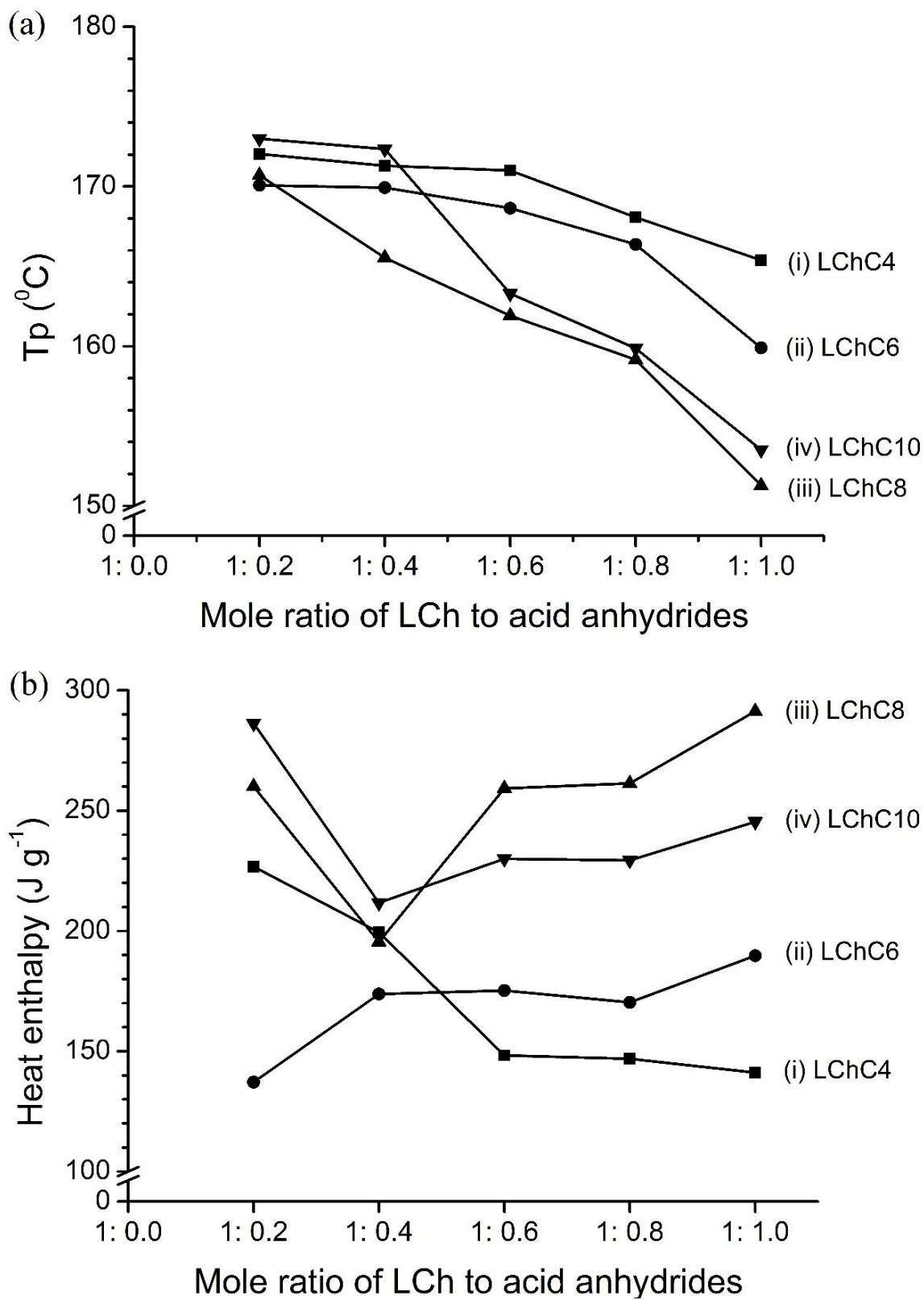
Fig. 7:   (a): Endothermic peak temperature and (b) heat enthalpy of endothermic peak of LChA at different mole ratio of LCh to acid anhydrides in DSC curve.

Kinematic viscosity

As shown in Fig. 8, it was found that the kinematic viscosity of LChA was slightly lower than LCh, this observation was in contrast to the dramatic increase in solution viscosity or gelation attributed to intermolecular aggregation of hydrophobically modified high molecular weight chitosans reported previously [30, 31]. This could be explained by the disruption of hydrogen bonding between polymer chains that increased the flexibility of LChA, diminishing their hydrodynamic volume in the solvent and hence reducing their viscosity [32]. The stronger hydrogen bonding in LCh as compared to LChA was reflected by aforementioned TGA analysis. This contributed to its higher stability and resistance towards heat. As temperature increased, the kinematic viscosity of both LCh and LChA decreased. The increase of temperature not only can increase the kinetic energy and flexibility of torsion angle of glycosidic linkage of chitosan [33], it also dehydrated the chitosan (decrease in hydrogen-bonded hydration water). The chitosan shrank and occupied smaller hydrodynamic volume, thereby enhancing their mobility to flow [34] and possibly promoting layer adhesion [35].

Field emission scanning electron microscope (FESEM)

Morphology of both LCh and LChA were observed using FESEM as presented in Fig. 9(a-e). LCh and LChA showed spherical particles with smooth but dented surface which was caused by the rapid evaporation of water via heating [36], in agreement with the observation of spray-dried chitosan microspheres by He, Davis [37] and Harris, Lecumberri [38]. From the size obtained from the average of at least 30 particles from several micrographs, the diameter of LCh was around 1 - 2 µm, the size did not differ significantly after acylated with butyryl groups. However, the acylation with longer hexanoyl groups caused the average size to increase to 4 - 5 µm. Further acylation resulted in LChC8 and LChC10 having the average size of 5 - 6 µm. The larger particle size of LChA acylated with longer acyl chains compared to those of shorter chains could be due to a larger occupancy volume of longer acyl groups. LCh (Fig. 9(a) and LChC4 (Fig. 9(b) with smaller particle size coalesced, this was presumably due to their smaller hydrodynamic volume that could promote layer adhesion during heating as discussed before in the kinematic viscosity section. The hollow capacity inside the core of LChA revealed the ability of the spherical particles to encapsulate drugs.
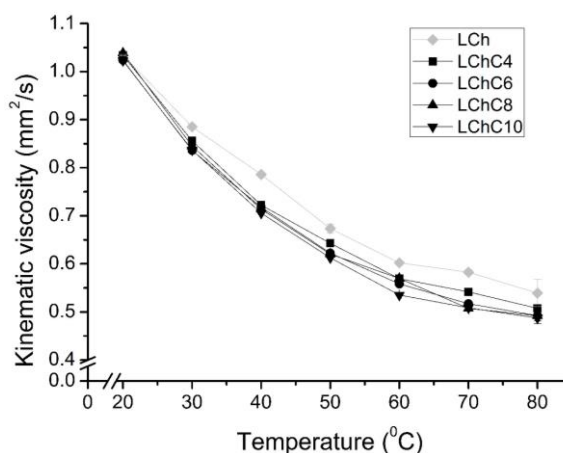
Fig. 8: Kinematic viscosity of LCh (◆), LChC4 (■), LChC6 (●), LChC8 (▲) and LChC10 (▼) from 20 to 80 °C.

(a)

(b)

(c)

(d)

(e)
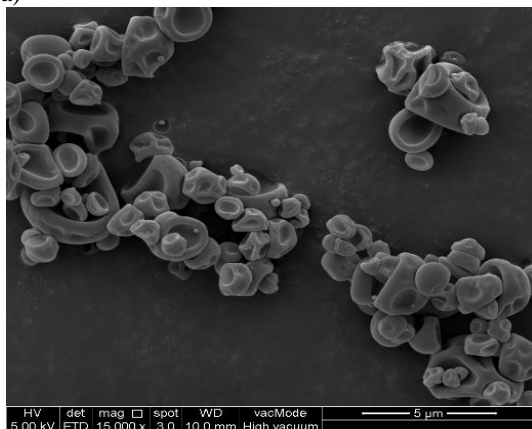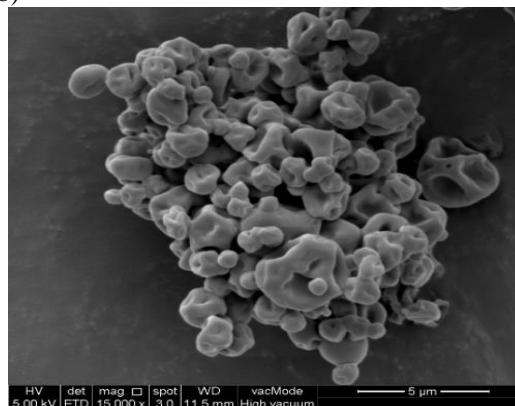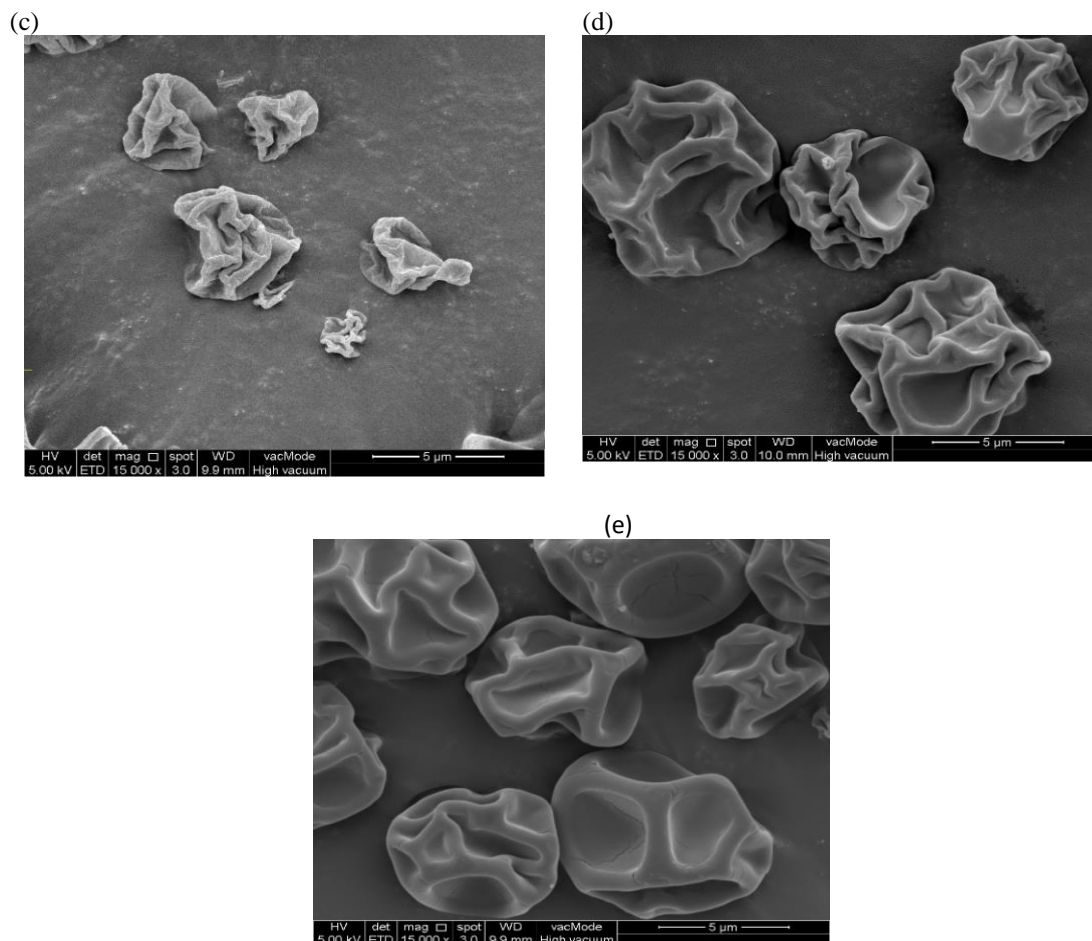
Fig. 9:　FESEM micrographs of (a) LCh, (b) LChC4, (c) LChC6, (d) LChC8 and (e) LChC10 under magnification at 15,000×, the scale bar shown was 5 µm.

Conclusions

The increment of DS was higher in short chains acylated chitosan compared to those of longer chains. The disruption of hydrogen bonding by the acyl groups resulted in higher sensitivity of LChA to moisture in TGA analysis. The weight loss of moisture was more prominent as DS and chain length of the LChA increased. This was supported by the decrease of endothermic peak temperature in DSC. The effect on the disruption of hydrogen bonding was also observed from the lower kinematic viscosity in LChA as a consequence of reducing hydrodynamic volume. The FESEM depicted the spherical shape and dented surface of LCh and LChA after being sprayed dry at high temperature, with the longer chain acylated chitosans exhibiting larger particle size and a core in which drugs could be encapsulated.

Acknowledgements

References

1. V. K. Mourya and N. N. Inamdar, Chitosan-Modifications and Applications: Opportunities Galore, *React. Funct. Polym.*, **68**, 1013 (2008).
2. M. Larsson, W. C. Huang, M. H. Hsiao, Y. J. Wang, M. Nyden, S. H. Chiou and D. M. Liu, Biomedical Applications and Colloidal Properties of Amphiphilically Modified Chitosan Hybrids, *Prog. Polym. Sci.*, **38**, 1307 (2013).

3. R. Mandke and J. Singh, Effect of Acyl Chain Length and Unsaturation on Physicochemical Properties and Transfection Efficiency of *N*-Acyl-Substituted Low-Molecular-Weight Chitosan, *J Pharm Sci*, **101**, 268 (2012).

4. F. Croisier and C. Jerome, Chitosan-Based Biomaterials for Tissue Engineering, *Eur. Polym. J.*, **49**, 780 (2013).

5. R. C. F. Cheung, T. B. Ng, J. H. Wong and W. Y. Chan, Chitosan: An Update on Potential Biomedical and Pharmaceutical Applications, *Mar. Drugs*, **13**, 5156 (2015).

6. Z. Liu, Y. Jiao, Y. Wang, C. Zhou, and Z. Zhang, Polysaccharides-Based Nanoparticles as Drug Delivery Systems, *Adv. Drug Del. Rev.*, **60**, 1650 (2008).

7. W. Wang, A. M. McConaghy, L. Tetley and I. F. Uchegbu, Controls on Polymer Molecular Weight may be Used to Control the Size of Palmitoyl Glycol Chitosan Polymeric Vesicles *Langmuir*, **17**, 631 (2001).

8. D. Li, X. Wang, Y. Guo, H. Huang and R. Sun, Preparation of Long-Chain Fatty Acyl-Grafted Chitosan in an Ionic Liquid and Their Self-Assembled Micelles in Water, *J. Macromol. Sci. B*, **51**, 2483 (2012).

9. L. Martin, C. G. Wilson, F. Koosha, L. Tetley, A. I. Gray, S. Senel and I. F. Uchegbu, The Release of Model Macromolecules may be Controlled by the Hydrophobicity of Palmitoyl Glycol Chitosan Hydrogels, *J. Control. Release*, **80**, 87 (2002).

10. V. Tangpasuthadol, N. Pongchaisirikul and V. P. Hoven, Surface Modification of Chitosan Films. Effects of Hydrophobicity on Protein Adsorption, *Carbohydr. Res.*, **338**, 937 (2003).

11. A. Neamnark, R. Rujiravanit and P. Supaphol, Electrospinning of Hexanoyl Chitosan, *Carbohydr. Polym.*, **66**, 298 (2006).

12. S. X. Tiew and M. Misran, Physicochemical Properties of Acylated Low Molecular Weight Chitosans, *Int. J. Polym. Mat. Polym. Biomat.*, p. 1 (2017).

13. J. Ahmed, In *Food and Biological Materials*, *Glass Transition and Phase Transitions*, John Wiley & Sons, Inc, New Jersey, US, p. 281 (2017).

14. F. A. A. Tirkistani, Thermal Analysis of Some Chitosan Schiff Bases, *Polym. Degrad. Stabil.*, **60**, 67 (1998).

15. X. Qu, A. Wirsen and A. C. Albertsson, Effect of Lactic/Glycolic Acid Side Chains on the Thermal Degradation Kinetics of Chitosan Derivatives, *Polymer*, **41**, 4841 (2000).

16. P. Katugampola and C. Winstead, Rheological Behavior and Thermal Stability of Palmitoyl Chitosan Varying the Degree of Substitution, *Int. J. Pharm. Sci. Invent*, **3**, 24 (2014).

17. C. Chen, S. Tao, X. Qiu, X. Ren and S. Hu, Long-Alkane-Chain Modified *N*-phthaloyl Chitosan Membranes with Controlled Permeability, *Carbohydr. Polym.*, **91**, 269 (2013).

18. C. Y. Choi, S. B. Kim, P. K. Pak, D. I. Yoo and Y. S. Chung, Effect of *N*-Acylation on Structure and Properties of Chitosan Fibers, *Carbohydr. Polym.*, **68**, 122 (2007).

19. C. Le Tien, M. Lacroix, P. Ispas-Szabo and M. A. Mateescu, *N*-acylated Chitosan: Hydrophobic Matrices for Controlled Drug Release, *J. Control. Rel.*, **93**, 1-13 (2003).

20. S. X. Tiew and M. Misran, Encapsulation of Salicylic Acid in Acylated Low Molecular Weight Chitosan for Sustained Release Topical Application, *J. Appl. Polym. Sci.*, **134**, Article no. 45273, 11 pg. (2017).

21. Y. Zhang, X. Zhang, R. Ding, J. Zhang and J. Liu, Determination of the Degree of Deacetylation of Chitosan by Potentiometric Titration Preceded by Enzymatic Pretreatment, *Carbohydr. Polym.*, **83**, 813 (2011).

22. R. Czechowska-Biskup, D. Jarosinska, B. Rokita, P. Ulanski and J. M. Rosiak, Determination of Degree of Deacetylation of Chitosan-Comarison of Methods, *Prog. Chem. Appl. Chitin Its Deriv.*, **17**, 5 (2012).

23. E. A. El-Hefian, E. S. Elgannoudi, A. Mainal, and A. H. Yahaya, Characterization of Chitosan in Acetic Acid: Rheological and Thermal Studies, *Turk. J. Chem.*, **34**, 47 (2010).

24. L. S. Guinesi and E. T. G. Cavalheiro, The Use of DSC curves to Determine the Acetylation Degree of Chitin/Chitosan Samples, *Thermochimica Acta*, **444**, 128 (2006).

25. E. A. El-Hefian, M. M. Nasef and A. H. Yahaya, Preparation and Characterization of Chitosan/Agar Blended Films: Part 2. Thermal, Mechanical, and Surface Properties, *E-J. Chem.*, **9**, 510 (2012).

26. M. Zeng, Z. Fang and C. Xu, Effect of Compatibility on the Structure of the Microporous Membrane Prepared by Selective Dissolution of Chitosan/Synthetic Polymer Blend Membrane, *J. Membr. Sci.*, **230**, 175 (2004).

27. W. Y. Chuang, T. H. Young, C. H. Yao and W. Y. Chiu, Properties of the Poly(vinyl alcohol)/Chitosan Blend and Its Effect on the Culture of Fibroblast *in vitro*, *Biomaterials*, **20**, 1479 (1999).

28. F. S. Kittur, K. V. Harish Prashanth, K. Udaya Sankar and R. N. Tharanathan, Characterization

of Chitin, Chitosan and Their Carboxymethyl Derivatives by Differential Scanning Calorimetry, *Carbohydr. Polym.*, **49**, 185 (2002).

29. H. Zhang, S. Yang, J. Fang, Y. Deng, D. Wang, and Y. Zhao, Optimization of the Fermentation Conditions of *Rhizopus Japonicus* M193 for the Production of Chitin Deacetylase and Chitosan, *Carbohydr. Polym.*, **101**, 57 (2014).

30. M. Rinaudo, R. Auzely, C. Vallin and I. Mullagaliev, Specific Interactions in Modified Chitosan Systems, *Biomacromolecules*, **6**, 2396 (2005).

31. Y. Y. Li, X. G. Chen, C. S. Liu, D. S. Cha, H. J. Park and C. M. Lee, Effect of the Molecular Mass and Degree of Substitution of Oleoylchitosan on the Structure, Rheological Properties, and Formation of Nanoparticles, *J. Agr. Food Chem.*, **55**, 4842 (2007).

32. Z. Zhang, X. Wang, M. Zhao and H. Qi, *O*-Acetylation of Low-Molecular-Weight Polysaccharide from *Enteromorpha Linza* with Antioxidant Activity, *Int. J. Biol. Macromol.*, **69**, 39 (2014).

33. M. A. Torres, M. M. Beppu and E. J. Arruda, Viscous and Viscoelastic Properties of Chitosan Solutions and Gels, *Braz J Food Technol*, **9**, 101 (2006).

34. D. P. Chattopadhyay and M. S. Inamdar, Aqueous Behavior of Chitosan, *Int. J. Polym. Sci.*, **2010**, Article ID 939536, 7 pg., (2010).

35. N. Seetapan, K. Mai-ngam, N. Plucktaveesak, and A. Sirivat, Linear Viscoelasticity of Thermoassociative Chitosan-g-poly(N-isopropylacrylamide) Polymer, *Rheologica Acta*, **45**, 1011 (2006).

36. A. Gharsallaoui, G. Roudaut, O. Chambin, A. Voilley and R. Saurel, Applications of Spray-Drying in Microencapsulation of Food Ingredients: An Overview, *Food Res. Int.*, **40**, 1107 (2007).

37. P. He, S. S. Davis and L. Illum, Chitosan Microspheres Prepared by Spray Drying, *Int. J. Pharm.*, **187**, 53 (1999).

38. R. Harris, E. Lecumberri, I. Mateos-Aparicio, M. Mengibar and A. Heras, Chitosan Nanoparticles and Microspheres for the Encapsulation of Natural Antioxidants Extracted from *Ilex Paraguariensis*, *Carbohydr. Polym.*, **84**, 803 (2011).